

## Research Article

# The Effects of MHD Flow and Heat Transfer for the UCM Fluid over a Stretching Surface in Presence of Thermal Radiation

M. Subhas Abel,<sup>1</sup> Jagadish V. Tawade,<sup>2</sup> and Jyoti N. Shinde<sup>3</sup>

<sup>1</sup> Department of Mathematics, Gulbarga University, Karnataka, Gulbarga 585 106, India

<sup>2</sup> Department of Mathematics, Walchand Institute of Technology, Maharashtra, Solapur 413006, India

<sup>3</sup> Department of Mathematics, Swamy Vivekananda Institute of Technology, Andhra Pradesh, Secunderabad 500 003, India

Correspondence should be addressed to Jagadish V. Tawade, jagadish.maths@yahoo.co.in

Received 10 March 2012; Revised 2 August 2012; Accepted 4 August 2012

Academic Editor: Ricardo Weder

Copyright © 2012 M. Subhas Abel et al. This is an open access article distributed under the Creative Commons Attribution License, which permits unrestricted use, distribution, and reproduction in any medium, provided the original work is properly cited.

An analysis is performed to investigate the effect of MHD and thermal radiation on the two-dimensional steady flow of an incompressible, upper-convected Maxwells (UCM) fluid in presence of external magnetic field. The governing system of partial differential equations are transformed into a system of coupled nonlinear ordinary differential equations and is solved numerically by efficient shooting technique. Velocity and temperature fields have been computed and shown graphically for various values of physical parameters. For a Maxwell fluid, a thinning of the boundary layer and a drop in wall skin friction coefficient is predicted to occur for the higher elastic number which agrees with the results of Hayat et al. 2007 and Sadeghy et al. 2006. The objective of the present work is to investigate the effect of elastic parameter  $\beta$ , magnetic parameter  $Mn$ , Eckert number  $Ec$ , Radiation parameter  $N$ , and Prandtl number  $Pr$  on flow and heat transfer characteristics.

## 1. Introduction

In recent years, the studies of boundary layer flows of Newtonian and non-Newtonian fluids over a stretching surface have received considerable attention because of their numerous applications in the field of metallurgy and chemical engineering and, particularly, in the extrusion of polymer sheet, from a die or in the drawing of plastic films. During the manufacture of these sheets, the melt issues from a slit and is subsequently stretched to achieve the desired thickness. Such investigations of magnetohydrodynamic (MHD) flow are very important industrially and have applications in different areas of research such as petroleum production and metallurgical processes. The magnetic field has been used in the process of purification of molten metals from nonmetallic inclusions. The study of flow and

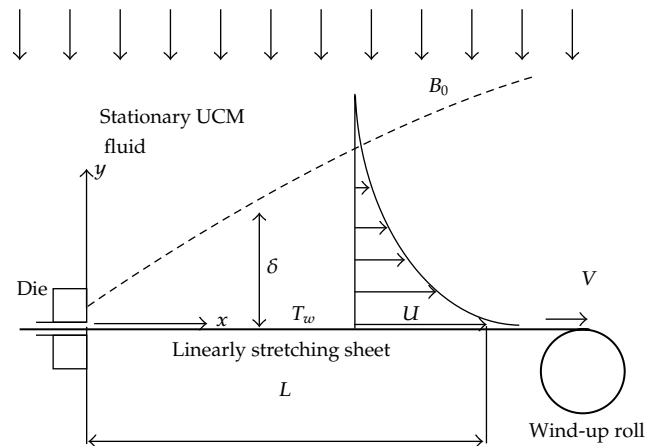


Figure 1: Schematic showing flow above a stretching sheet.

heat transfer caused by a stretching surface is of great importance in many manufacturing processes such as in extrusion process, glass blowing, hot rolling, manufacturing of plastic and rubber sheets, crystal growing, continuous cooling, and fibers spinning. Water is amongst the most widely used coolant liquid. In all these cases, a study of flow field and heat transfer can be of significant importance because the quality of the final product depends to a large extent on the skin friction coefficient and the surface heat transfer rate [1].

Sarpakaya [2] was the first researcher to study the MHD flow of a non-Newtonian fluid. Prandtl's boundary layer theory proved to be of great use in Newtonian fluids as Navier-Stokes equations can be converted into much simplified boundary layer equation which is easier to handle.

Crane [3] was the first among others to consider the steady two-dimensional flow of a Newtonian fluid driven by a stretching elastic flat sheet which moves in its own plane with a velocity varying linearly with the distance from a fixed point. Subsequently, various aspects of the flow and/or heat transfer problems for stretching surfaces moving in the finite fluid medium have been explored in many investigations, for example, [4–13].

Extrusion of molten polymers through a slit die for the production of plastic sheets is an important process in polymer industry. The operation normally involves significant heat transfer between the sheet and the surrounding fluid, thus making it a thermofluid mechanical problem to address [14]. In a typical sheet production process the extrudate starts to solidify as soon as it exits from the die. The sheet is then brought into a required shape by a wind-up roll upon solidification (see Figure 1). An important aspect of the flow is the extensibility of the sheet which can be employed effectively to improve its mechanical properties along the sheet. To further improve sheet mechanical properties, it is necessary to control its cooling rate. Physical properties of the cooling medium, for example, its thermal conductivity, can play a decisive role in this regard [14]. The success of the whole operation can be argued to depend also on the rheological properties of the fluid above the sheet as it is the fluid viscosity which determines the (drag) force required to pull the sheet.

Generally it is observed that rheological properties of a material are specified by their constitutive equations. The simplest constitutive equation for a fluid is a Newtonian one, and the governing equation for such a fluid is the Navier-Stokes equation. But in many fields, such as food industry, drilling operations, and bioengineering, the fluids, rather synthetic or natural or mixtures of different stuffs such as water, particles, oils, red cells, and other long

chain of molecules. This combination imparts strong non-Newtonian characteristics to the resulting liquids. In these cases, the fluids have been treated as non-Newtonian fluids.

Problems involving fluid flow over a stretching sheet can be found in many manufacturing processes such as polymer extrusion, wire and fibre coating, and foodstuff processing. Essentially, the quality of the final product depends on the rate of cooling in the process which is significantly influenced by the fluid flow and heat transfer mechanism. Water is amongst the most-widely used fluids to be used as the cooling medium. However, the rate of cooling achievable with water is often realized to be too excessive for certain sheet materials. To have a better control on the rate of cooling, in recent years it has been proposed that it might be advantageous for water to be made more or less viscoelastic, say, through the use of polymeric additives [15, 16]. The idea is to alter flow kinematics in such a way that it leads to a slower rate of solidification with the price being paid that fluid's viscosity is normally increased by such additives. A better and less intuitive idea is to rely on a transverse magnetic field for affecting flow kinematics provided that the fluid is electrically conducting [17]. The radiative heat transfer properties of the cooling medium may also be manipulated to judiciously influence the rate of cooling [18, 19]. In recent years, MHD flows of viscoelastic fluids above stretching sheets (with and without heat transfer involved) have also been addressed by various researchers [20–23].

A non-Newtonian second-grade fluid does not give meaningful results for highly elastic fluids (polymer melts) which occur at high Deborah numbers [24, 25]. Therefore, the significance of the results reported in the above works is limited, at least as far as polymer industry is concerned. Obviously, for the theoretical results to become of any industrial significance, more realistic viscoelastic fluid models such as upper-convected Maxwell model or Oldroyd-B model should be invoked in the analysis. Indeed, these two fluid models have recently been used to study the flow of viscoelastic fluids above stretching and nonstretching sheets but with no heat transfer effects involved [26–28].

Some researchers [27, 29–31] have done the work related to UCM fluid by using HAM-method, and the researcher [28] have studied UCM fluid by using numerical methods for only to solve the equation of motion but not for the heat transfer.

Motivated by all the above works, it is interested to extend the research work carried out by the researchers Hayat et al. [24] and Sadeghy et al. [29] in which the velocity field above the sheet was calculated for MHD flow of a Maxwell fluid with no heat transfer involved using homotopy analysis method (HAM). The effect of thermal radiation on MHD flow of Maxwellian fluids above the stretching sheets has been investigated by Aliakbar et. al [31] by using homotopy analysis method (HAM). It is recognized that there are many other methods that could be considered in order to describe some reasonable solutions for this particular type of problem. But to the best of our knowledge, no numerical solution has previously been investigated for such type of problems even having various applications in engineering processes involving nuclear reactors, gas turbines, power production, and solar collectors, the cooling of electronic equipments and polymer industry. So, the aim of this study is to analyze, numerically, the combined effect of thermal radiation and viscous dissipation on steady MHD flow and heat transfer of an upper-convected Maxwell fluid past a stretching sheet in presence of external magnetic field.

## 2. Formulation of the Problem

The equations governing the transfer of heat and momentum between a stretching sheet and the surrounding fluid (see Figure 1) can be significantly simplified if it can be assumed that

boundary layer approximations are applicable to both momentum and energy equations. Although this theory is incomplete for viscoelastic fluids, but has been discussed by Renardy [27], it is more plausible for Maxwell fluids as compared to other viscoelastic fluid models for MHD flow of an incompressible Maxwell fluid resting above a stretching sheet. The steady two-dimensional boundary layer equations for the fluid can be written as [25, 26]

$$\frac{\partial u}{\partial x} + \frac{\partial v}{\partial y} = 0, \quad (2.1)$$

$$u \frac{\partial u}{\partial x} + v \frac{\partial u}{\partial y} + \lambda \left[ u^2 \frac{\partial^2 u}{\partial x^2} + v^2 \frac{\partial^2 u}{\partial y^2} + 2uv \frac{\partial^2 u}{\partial x \partial y} \right] = \nu \frac{\partial^2 u}{\partial y^2} - \frac{\sigma B_0^2}{\rho} u, \quad (2.2)$$

where  $B_0$  is the strength of the magnetic field,  $\nu$  is the kinematic viscosity of the fluid, and  $\lambda$  is the relaxation time Parameter of the fluid. As to the boundary conditions, we are going to assume that the sheet is being stretched linearly. Therefore the appropriate boundary conditions on the flow are

$$u = Bx, \quad v = 0 \quad \text{at } y = 0, \quad u \longrightarrow 0 \text{ as } y \longrightarrow \infty, \quad (2.3)$$

where  $B > 0$  is the stretching rate. Here  $x$  and  $y$  are, respectively, the directions along and perpendicular to the sheet, and  $u$  and  $v$  are the velocity components along  $x$  and  $y$  directions. The flow is caused solely by the stretching of the sheet, the free stream velocity being zero. Equations (2.1) and (2.2) admit a self-similar solution of the following form:

$$u = Bx f'(\eta), \quad v = \sqrt{\nu B} f(\eta), \quad \eta = \left( \frac{B}{\nu} \right)^{1/2} y, \quad (2.4)$$

where superscript (') denotes the differentiation with respect to  $\eta$ . Clearly  $u$  and  $v$  satisfy (2.1) identically. Substituting these new variables in (2.2), we have

$$f''' - M^2 f' - (f')^2 + f'' + \beta (2f f' f'' - f f''') = 0. \quad (2.5)$$

Here  $M^2 = \sigma B_0^2 / \rho B$  and  $\beta = \lambda B$  are magnetic and elastic parameters.

The boundary conditions (2.3) become

$$\begin{aligned} f'(0) &= 1, & f(0) &= 0 \quad \text{at } \eta = 0 \\ f'(\infty) &\longrightarrow 0, & f''(0) &\longrightarrow 0 \quad \text{as } \eta \longrightarrow \infty. \end{aligned} \quad (2.6)$$

### 3. Heat Transfer Analysis

By using usual boundary layer approximations, the equation of the energy for two-dimensional flow is given by

$$u \frac{\partial T}{\partial x} + v \frac{\partial T}{\partial y} = \frac{k}{\rho C_p} \frac{\partial^2 T}{\partial y^2} + \frac{\mu}{\rho C_p} \left( \frac{\partial u}{\partial y} \right)^2 - \frac{1}{\rho C_p} \left( \frac{\partial q_r}{\partial y} \right), \quad (3.1)$$

where  $T$ ,  $\rho$ ,  $c_p$ , and  $k$  are, respectively, the temperature, the density, specific heat at constant pressure and the thermal conductivity is assumed to vary linearly with temperature. Following Rosseland approximation (see [32]) the radiative heat flux  $q_r$  and is modeled as

$$\frac{\partial q_r}{\partial y} = -\frac{4\sigma^*}{3k^*} \frac{\partial(T^4)}{\partial y}, \quad (3.2)$$

where  $\sigma^*$  is the Stefan-Boltzmann constant, and  $k^*$  is the mean absorption coefficient. Assuming that the differences in temperature within the flow are such that  $T^4$  can be expressed as a linear combination of the temperature, we expand  $T^4$  in a Taylor's series about  $T_\infty$  as follows:

$$T^4 = T_\infty^4 + 4T_\infty^3(T - T_\infty) + 6T_\infty^2(T - T_\infty)^2 + \dots, \quad (3.3)$$

and, neglecting higher order terms beyond the first degree in  $(T - T_\infty)$ , we get

$$T^4 \cong -3T_\infty^4 + 4T_\infty^3 T. \quad (3.4)$$

Substituting (3.4) into (3.2), we obtain

$$\frac{\partial q_r}{\partial y} = -\frac{16T_\infty^* \sigma^*}{3k^*} \frac{\partial^2 T^4}{\partial y^2}. \quad (3.5)$$

Using (3.5) in (3.1) we obtain

$$\begin{aligned} u \frac{\partial T}{\partial x} + v \frac{\partial T}{\partial y} &= \frac{k}{\rho C_p} \frac{\partial^2 T}{\partial y^2} + \frac{\mu}{\rho C_p} \left( \frac{\partial u}{\partial y} \right)^2 - \frac{1}{\rho C_p} \left( -\frac{16T_\infty^* \sigma^*}{3k^*} \frac{\partial^2 T^4}{\partial y^2} \right) \\ \frac{\partial T}{\partial t} + u \frac{\partial T}{\partial x} + v \frac{\partial T}{\partial y} &= \frac{k}{\rho C_p} \frac{\partial^2 T}{\partial y^2} + \frac{\mu}{\rho C_p} \left( \frac{\partial u}{\partial y} \right)^2 + \frac{q'''}{\rho c_p} - \frac{1}{\rho c_p} \left( -\frac{16T_\infty^* \sigma^*}{3k^*} \frac{\partial^2 T^4}{\partial y^2} \right). \end{aligned} \quad (3.6)$$

We define the dimensionless temperature as

$$\theta(\eta) = \frac{T - T_\infty}{T_w - T_\infty}, \quad \text{where } T_w - T_\infty = b \left( \frac{x}{l} \right)^2 \theta(\eta) \quad (\text{PST Case}) \quad (3.7)$$

$$g(\eta) = \frac{T - T_\infty}{b(x/l)^2(1/k)\sqrt{v/b}}, \quad \text{where } T_w - T_\infty = \frac{D}{k} \left( \frac{x}{l} \right)^2 \sqrt{\frac{v}{b}} \quad (\text{PHF Case}). \quad (3.8)$$

**Table 1:** Comparison of values of skin friction coefficient  $-f''(0)$  with  $M = 0.0$  and  $M = 0.2$ .

$\beta$	Sadeghy et al. [29] Hayat et al. [24]			Present results	
	$M = 0.0$	$M = 0.0$	$M = 0.2$	$M = 0.0$	$M = 0.2$
0.0	1.00000	1.90250	1.94211	0.999962	1.095445
0.4	1.10084	2.19206	2.23023	1.101850	1.188270
0.8	1.19872	2.50598	2.55180	1.196692	1.275878
1.2	—	2.89841	2.96086	1.285257	1.358733
1.6	—	3.42262	3.51050	1.368641	1.437369
2.0	—	4.13099	4.25324	1.447617	1.512280

**Table 2:** Comparison of values of Eckert number Ec and magnetic parameter Mn in PST case ( $\lambda = 0.1, Pr = 3, N = 30$ ).

Ec	Mn	Aliakbar et al. [31] Present results	
		$-\theta'(0)$	$-\theta'(0)$
0.0	0.0	2.47116	2.439162
5.0	0.0	-1.38806	-1.753606
10.0	0.0	-5.24982	-5.938303
0.0	0.0	2.47116	2.439162
0.0	10.0	1.0472	1.927487
0.0	20.0	0.730305	1.738464

The thermal boundary conditions depend upon the type of the heating process being considered. Here, we are considering two general cases of heating, namely, (1) prescribed surface temperature and (2) prescribed wall heat flux, varying with the distance.

### 3.1. Governing Equation for the Prescribed Surface Temperature Case

For this heating process, the prescribed temperature is assumed to be that a quadratic function of  $x$  is given by

$$\begin{aligned}
 u = Bx, \quad v = 0, \quad T = T_w(x) = T_0 - T_s \left( \frac{x}{l} \right)^2 \quad \text{at } y = 0. \\
 u = 0, \quad T \rightarrow T_\infty \quad \text{as } y \rightarrow \infty,
 \end{aligned} \tag{3.9}$$

where  $l$  is the characteristic length. Using (2.4), (3.1), and (3.9), the dimensionless temperature variable  $\theta$ , given by (3.7), satisfies the following:

$$\text{Pr} \left[ 2f'\theta - \theta'f - \text{Ec}f''^2 \right] \frac{3N}{3N+4} = \theta'', \tag{3.10}$$

**Table 3:** Values of surface temperature  $\theta(1)$  and heat transfer rate  $-\theta'(0)$  for various values of Mn, Pr, Ec,  $N$ , and  $\beta$ .

Pr	Mn	Ec	$N$	$\beta$	$\theta(1)$	$-\theta'(0)$
1.0	0.5	1.0	30.0	0.1	-0.000000	0.756603
5.0	0.5	1.0	30.0	0.1	0.000000	1.501049
10.0	0.5	1.0	30.0	0.1	-0.000000	1.889985
3.0	0.0	1.0	30.0	0.1	0.000000	1.593204
3.0	5.0	1.0	30.0	0.1	0.000001	-1.206756
3.0	10.0	1.0	30.0	0.1	0.000000	-3.367022
3.0	0.5	0.0	30.0	0.1	0.000001	2.385235
3.0	0.5	1.0	30.0	0.1	0.000001	1.242008
3.0	0.5	2.0	30.0	0.1	-0.000001	0.098781
3.0	0.5	1.0	1.0	0.1	0.000000	0.876908
3.0	0.5	1.0	30.0	0.1	0.000001	1.242008
3.0	0.5	1.0	30.0	0.0	0.000000	1.287680
3.0	0.5	1.0	30.0	0.1	0.000001	1.242008
3.0	0.5	1.0	30.0	0.3	-0.000001	1.150961

where  $Pr = \mu c_p / k$  is the Prandtl number,  $Ec = a^2 l^2 / C_p T_s$  is the Eckert number, and  $N = 4\sigma^* T_\infty^3 / k k^*$  is the thermal radiation parameter. The corresponding boundary conditions are

$$\begin{aligned}\theta(0) &= 1 \quad \text{at } \eta = 0 \\ \theta(\infty) &= 0 \quad \text{as } \eta \rightarrow \infty.\end{aligned}\tag{3.11}$$

### 3.2. Governing Equation for the Prescribed Heat Flux Case

The power law heat flux on the wall surface is considered to be a quadratic power of  $x$  in the following form:

$$\begin{aligned}u &= Bx, \quad -k \left( \frac{\partial T}{\partial y} \right)_w = q_w = b \left( \frac{x}{l} \right)^2 \quad \text{at } y = 0 \\ u &\rightarrow 0, \quad T \rightarrow T_\infty \quad \text{as } y \rightarrow \infty.\end{aligned}\tag{3.12}$$

Here  $D$  is constant. Using (2.4), (3.1), and (3.12), the dimensionless temperature variable  $g$ , given by (3.2), satisfies the following:

$$Pr \left[ 2f'g - g'f - Ec f''^2 \right] \frac{3N}{3N+4} = g''.\tag{3.13}$$

The corresponding boundary conditions are

$$g'(\eta) = -1, \quad g(\infty) = 0.\tag{3.14}$$

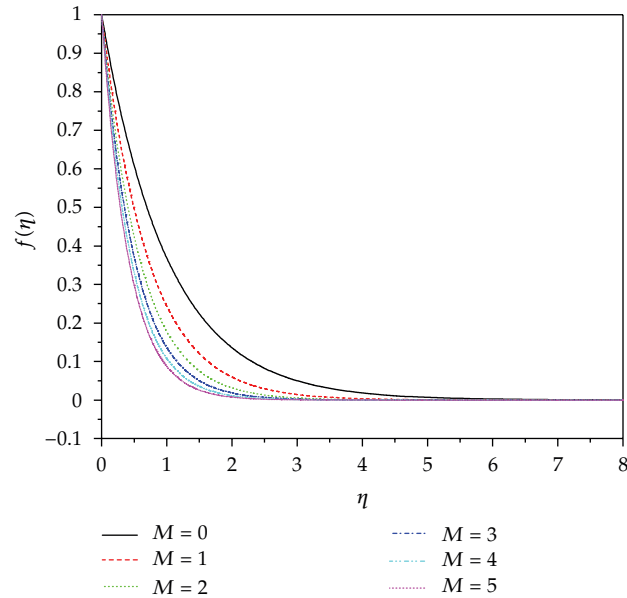


**Figure 2:** The effect of MHD parameter  $Mn$  on  $u$ -velocity component  $f$  at  $\beta = 0$ .

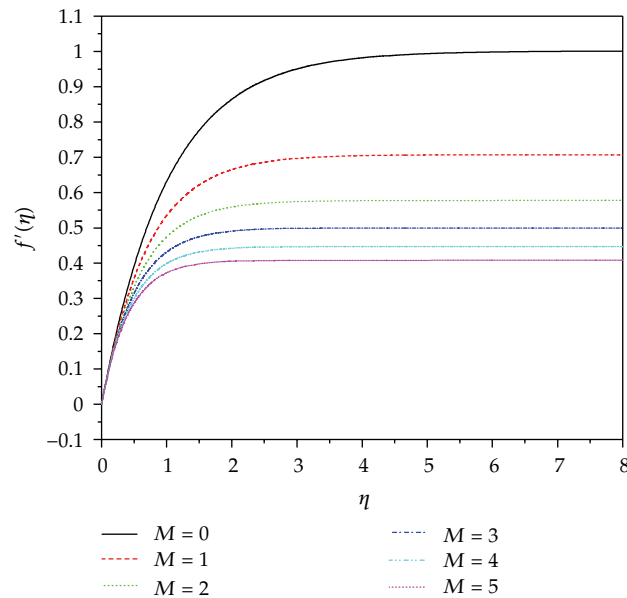


**Figure 3:** The effect of MHD parameter  $Mn$  on  $v$ -velocity component  $f'$  at  $\beta = 0$ .

The rate of heat transfer between the surface and the fluid conventionally expressed in dimensionless form as a local Nusselt number is given by

$$Nu_x \equiv -\frac{x}{T_w - T_\infty} \left( \frac{\partial T}{\partial y} \right)_{y=0} = -x\sqrt{\text{Re}} \theta'(0). \quad (3.15)$$



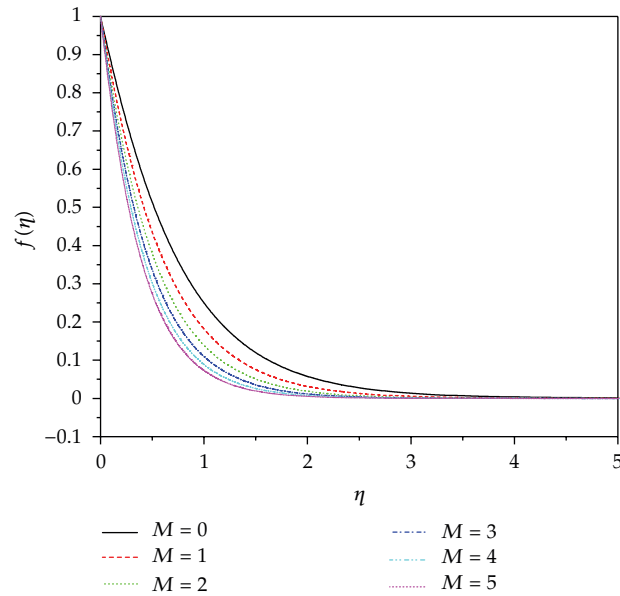


Figure 4: The effect of MHD parameter Mn on  $u$ -velocity component  $f$  at  $\beta = 1$ .

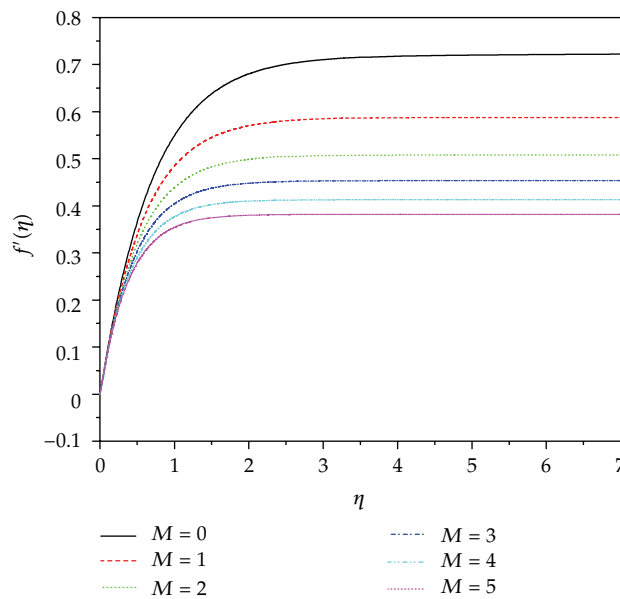


Figure 5: The effect of MHD parameter Mn on  $v$ -velocity component  $f'$  at  $\beta = 1$ .

Similarly, momentum equation is simplified, and exact analytic solutions can be derived for the skin-friction coefficient or frictional drag coefficient as

$$C_f \equiv \frac{(\mu(\partial u / \partial y))_{y=0}}{\rho(Bx)^2} = -f''(0) \frac{1}{\sqrt{\text{Re}_x}}, \tag{3.16}$$

where  $\text{Re}_x = \rho Bx^2 / \mu$  is known as local Reynolds number.

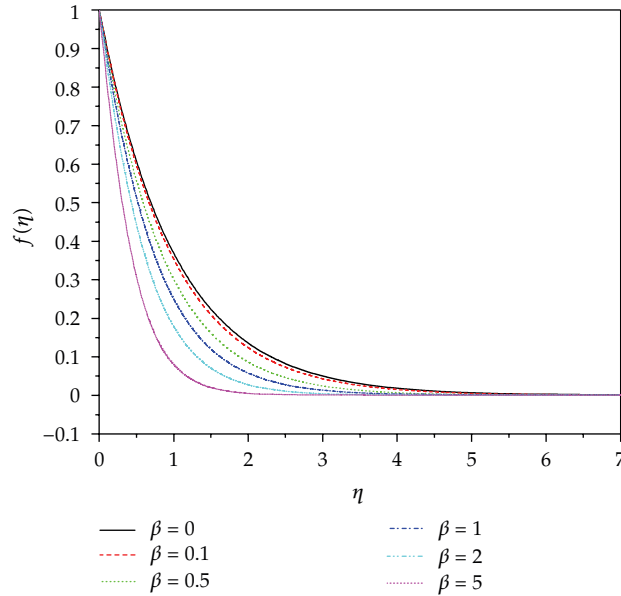


Figure 6: The effect of elastic parameter  $\beta$  on  $u$ -velocity component  $f$  at  $Mn = 0$ .

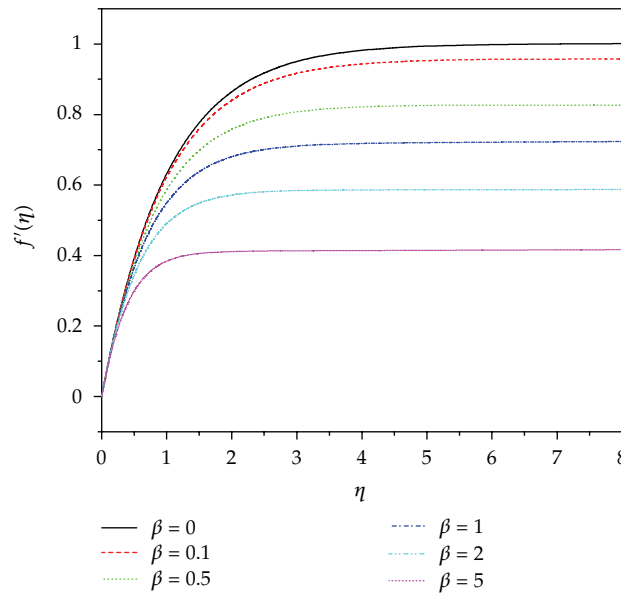


Figure 7: The effect of elastic parameter  $\beta$  on  $v$ -velocity component  $f'$  at  $Mn = 0$ .

#### 4. Numerical Solution

We adopt the most effective shooting method (see [33, 34]) with fourth-order Runge-Kutta integration scheme to solve boundary value problems in PST and PHF cases mentioned in

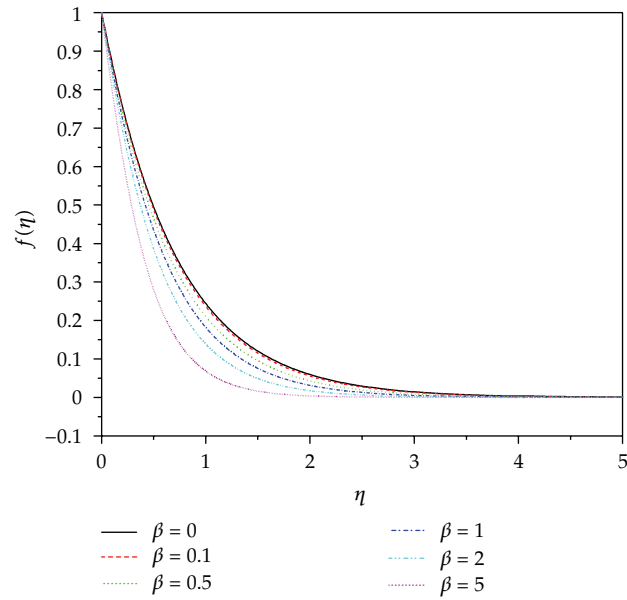


Figure 8: The effect of elastic parameter  $\beta$  on  $u$ -velocity component  $f$  at  $Mn = 1$ .

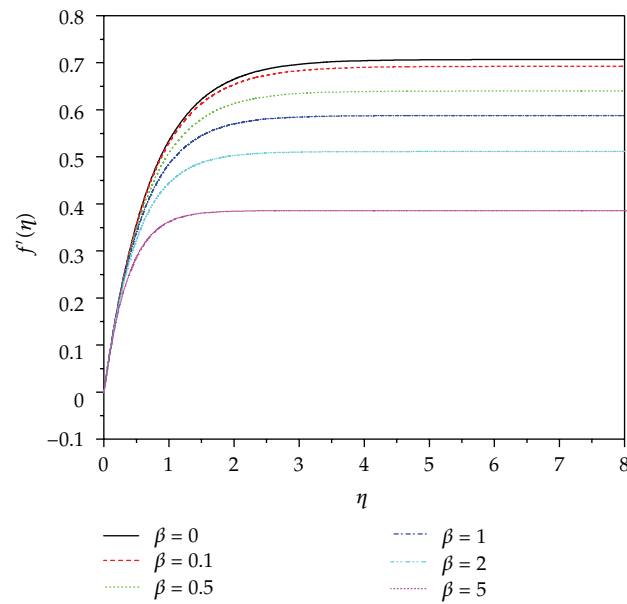
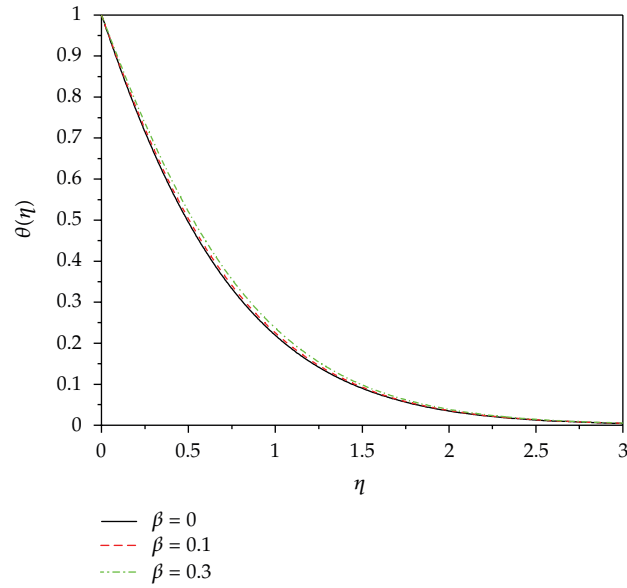
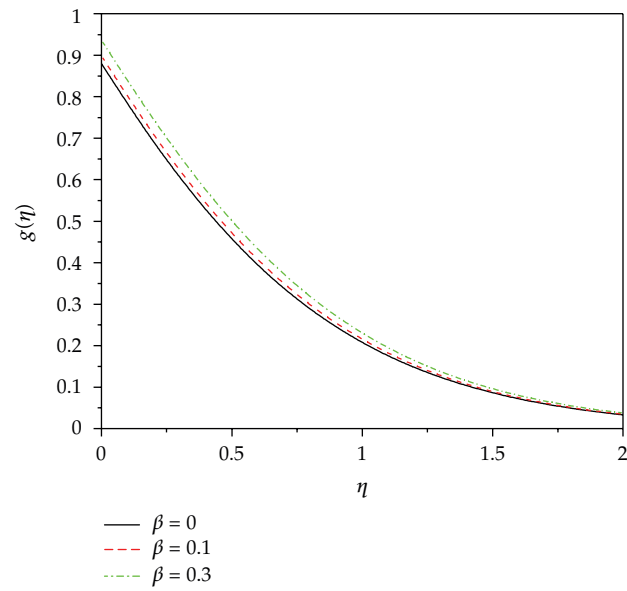


Figure 9: The effect of elastic parameter  $\beta$  on  $u$ -velocity component  $f'$  at  $Mn = 1$ .



**Figure 10:** The effect of elastic parameter  $\beta$  on the temperature profile for the PST case at  $Mn = 0.5$ ,  $Ec = 1$ ,  $Pr = 3$ ,  $N = 30$ .



**Figure 11:** The effect of elastic parameter  $\beta$  on the temperature profile for the PHF case at  $Mn = 0.5$ ,  $Ec = 1$ ,  $Pr = 3$ ,  $N = 30$ .

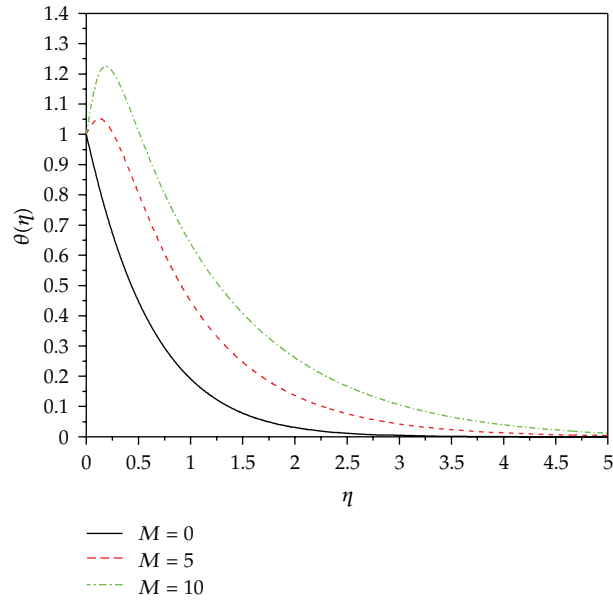


**Figure 12:** The effect of magnetic parameter Mn on the temperature profile for the PST case at  $\beta = 0.1$ ,  $Ec = 1$ ,  $Pr = 3$ ,  $N = 30$ .

the previous section. The nonlinear equations (2.5) and (3.10) in the PST case are transformed into a system of five first-order differential equations as follows:

$$\begin{aligned}
 \frac{df_0}{d\eta} &= f_1, \\
 \frac{df_1}{d\eta} &= f_2, \\
 \frac{df_2}{d\eta} &= \frac{(f_1)^2 + M^2 f_1 - f_0 f_2 - 2\beta f_0 f_1 f_2}{1 - \beta f_0^2}, \\
 \frac{d\theta_0}{d\eta} &= \theta_1, \\
 \frac{d\theta_1}{d\eta} &= Pr \left[ 2f_1 \theta_0 - \theta_1 f_0 - Ec f''^2 \right] \frac{3N}{3N + 4}.
 \end{aligned}
 \tag{4.1}$$

Subsequently the boundary conditions in (2.6) and (3.11) take the following form:

$$\begin{aligned}
 f_0(0) = 0, \quad f_1(0) = 1, \quad f_1(\infty) = 0, \\
 f_2(0) = 0, \quad \theta_0(0) = 0, \quad \theta_0(\infty) = 0.
 \end{aligned}
 \tag{4.2}$$

Here  $f_0 = f(\eta)$  and  $\theta_0 = \theta(\eta)$ , aforementioned boundary value problem, is first converted into an initial value problem by appropriately guessing the missing slopes  $f_2(0)$

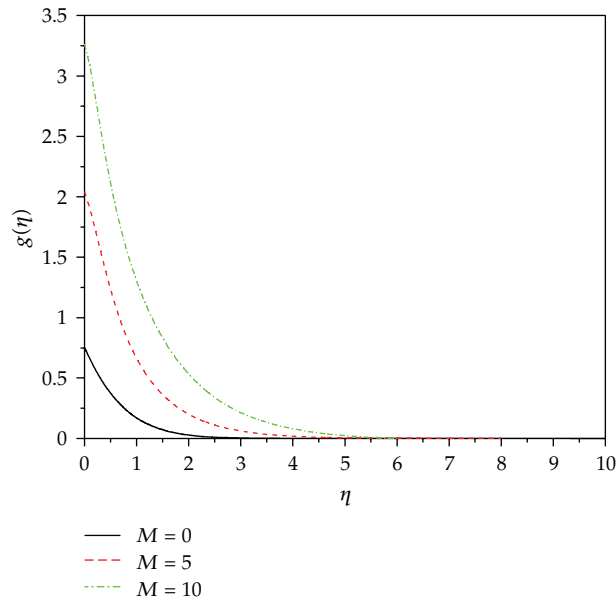


**Figure 13:** The effect of magnetic parameter  $Mn$  on the temperature profile for the PHF case at  $\beta = 0.1$ ,  $Ec = 1$ ,  $Pr = 3$ ,  $N = 30$ .

and  $\theta_1(0)$ . The resulting IVP is solved by shooting method for a set of parameters appearing in the governing equations with a known value of  $f_2(0)$  and  $\theta_1(0)$ . The convergence criterion largely depends on fairly good guesses of the initial conditions in the shooting technique. The iterative process is terminated until the relative difference between the current iterative values of  $f_2(0)$  matches with the previous iterative value of  $f_2(0)$  up to a tolerance of  $10^{-6}$ . Once the convergence is achieved, we integrate the resultant ordinary differential equations using standard fourth-order Runge-Kutta method with the given set of parameters to obtain the required solution.

## 5. Results and Discussion

The nonlinear coupled ordinary differential equations (2.5), (3.10), and (3.13) subject to the boundary conditions (2.6), (3.11), and (3.14) were solved numerically using the most effective numerical fourth-order Runge-Kutta method with efficient shooting technique. Appropriate similarity transformation is adopted to transform the governing partial differential equations of flow and heat transfer into a system of nonlinear ordinary differential equations. In order to validate the numerical method, comparison with the exact analytical solutions for the local skin-friction and the local Nusselt number is shown in Tables 1 and 2. Without any doubt, from these tables, we can claim that our results are in excellent agreement with that of references Hayat et al. [24], Sadeghy et al. [29], and Aliakbar et al. [31] under some limiting cases. The effects of surface temperature  $\theta(1)$  and heat transfer rate  $-\theta'(0)$  for various values of  $Mn$ ,  $Pr$ ,  $Ec$ ,  $N$ , and  $\beta$  are tabulated in Table 3. The effect of several parameters controlling the velocity and temperature profiles is shown graphically and discussed briefly.

Figures 2 and 3 reveal that, for  $\beta = 0$  the effect of magnetic parameter  $Mn$  on the velocity profile above the sheet. It is clear that increasing values of  $Mn$  leads decrease of

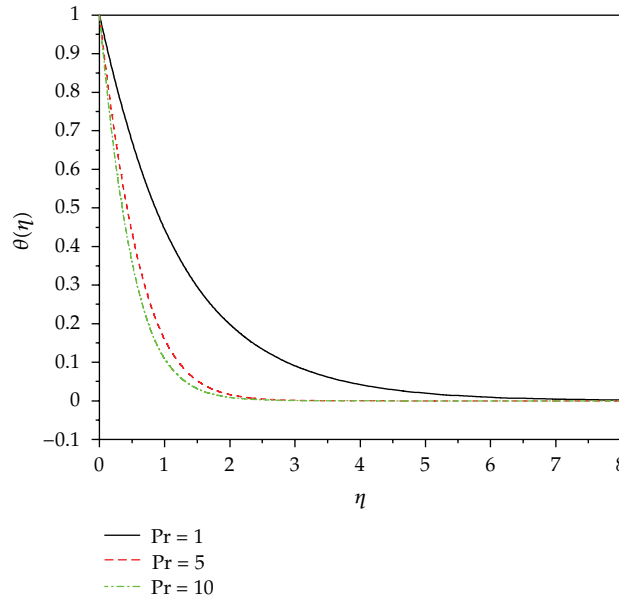


**Figure 14:** The effect of Prandtl number  $Pr$  on the temperature profile for the PST case at  $\beta = 0.1$ ,  $Mn = 0.5$ ,  $Ec = 1$ ,  $N = 30$ .

both  $u$ - and  $v$ -velocity components at any given point above the sheet. This is due to the fact that applied transverse magnetic field produces a drag in the form of Lorentz force thereby decreasing the magnitude of velocity. The drop in horizontal velocity as a consequence of increase in the strength of magnetic field is observed. Figures 4 and 5 show the same effect as said above for  $\beta = 1$ . That is, an increase in  $Mn$  leads decrease of fluid velocity at any given point above the sheet.

Figures 6 and 7 show the effect of elastic parameter  $\beta$  for  $Mn = 0$  on the velocity profile above the sheet. An increase in the elastic parameter is noticed to decrease both  $u$ - and  $v$ -velocity components at any given point above the sheet. Figures 8 and 9 show the effect of elastic parameter  $\beta$  on the velocity profiles above the sheet. An increase in the elastic number  $\beta$  is seen to decrease both  $u$ - and  $v$ -velocity components at any given point above sheet. A decrease in a stream-wise velocity component,  $u$ , can result in a decrease in the amount of heat transferred from the sheet to the fluid. Similarly, a decrease in the transverse velocity component,  $v$ , means that the amount of fresh fluid which is extended from the low-temperature region outside the boundary layer and directed towards the sheet is reduced thus decreasing the amount of heat transfer. The two effects are in the same direction reinforcing each other. Thus, an increase in the elastic number is expected to decrease the total amount of heat transfer from the sheet to the fluid, as suggested by Figures 10 and 11. That is, an increase in the elastic number decreases fluid temperature at any given point above the sheet.

Figures 12 and 13 show the effect of magnetic parameter on the temperature profiles above the sheet for both PST and PHF cases. An increase in the magnetic parameter is seen to increase the fluid temperature  $\theta(\eta)$  above the sheet. That is, the thermal boundary layer becomes thicker for larger the magnetic parameter.

Figures 14 and 15 show the effect of Prandtl number on the temperature profiles above the sheet for both PST and PHF cases. An increase in the Prandtl number is seen to decrease

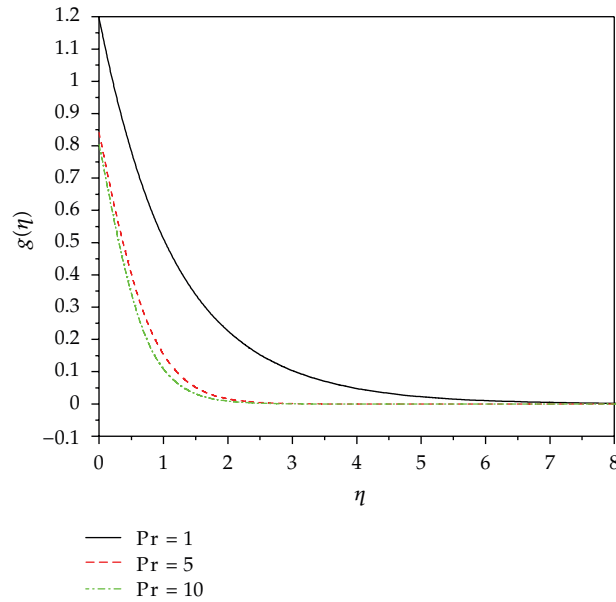


**Figure 15:** The effect of Prandtl number  $Pr$  on the temperature profile for the PHF case at  $\beta = 0.1$ ,  $Mn = 0.5$ ,  $Ec = 1$ ,  $N = 30$ .

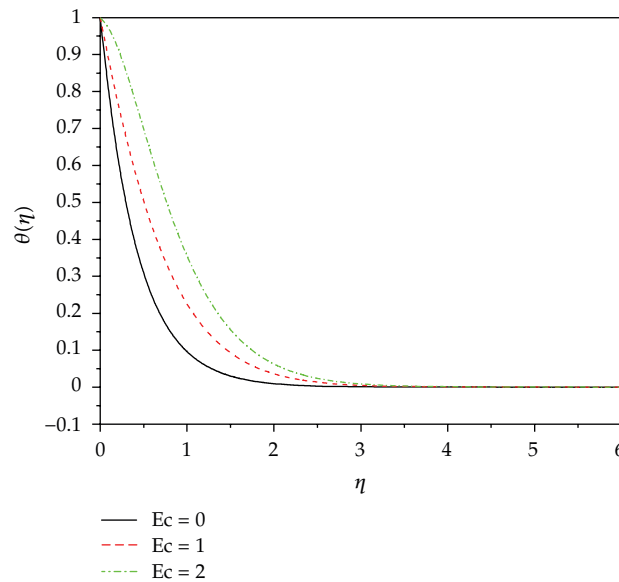


**Figure 16:** The effect of Eckert number  $Ec$  on the temperature profile for the PST case at  $\beta = 0.1$ ,  $Mn = 0.5$ ,  $Pr = 3$ ,  $N = 30$ .

the fluid temperature  $\theta(\eta)$  above the sheet. That is not surprising realizing the fact that the thermal boundary becomes thinner for larger the Prandtl number. Therefore, with an increase in the Prandtl number the rate of thermal diffusion drops. This scenario is valid for both PST and PHF cases. For the PST case the dimensionless wall temperature is unity for all parameter



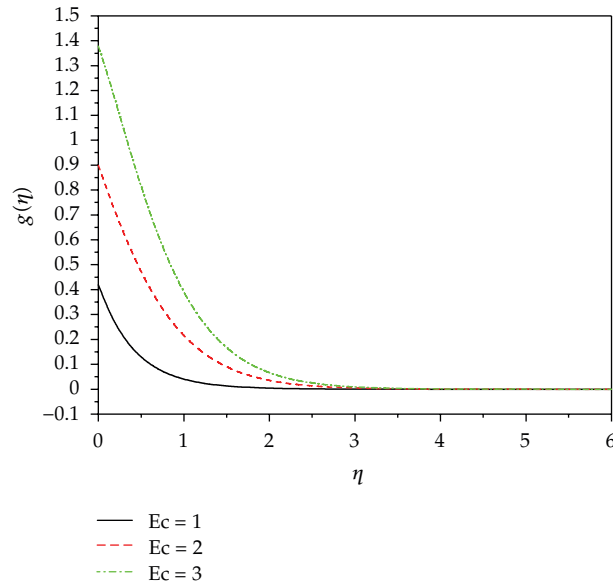


**Figure 17:** The effect of Eckert number  $Ec$  on the temperature profile for the PHF case at  $\beta = 0.1$ ,  $Mn = 0.5$ ,  $Pr = 3$ ,  $N = 30$ .

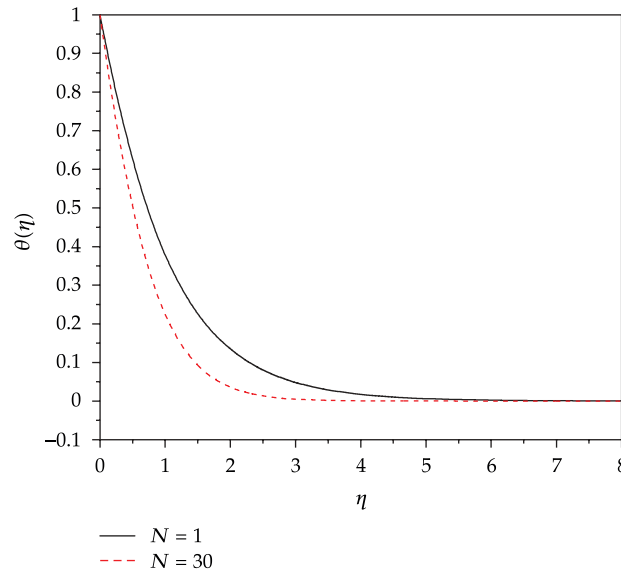


**Figure 18:** The effect of radiation parameter  $N$  on the temperature profile for the PST case at  $\beta = 0.1$ ,  $Mn = 0.5$ ,  $Ec = 1$ ,  $Pr = 3$ .

values. However, it may be other than unity for the PHF case because of its differing thermal boundary conditions.

Figures 16 and 17 show the effect of Eckert number on the temperature profiles above the sheet for both PST and PHF cases. An increase in the value of Eckert number is seen to increase the temperature of the fluid at any point above the sheet.

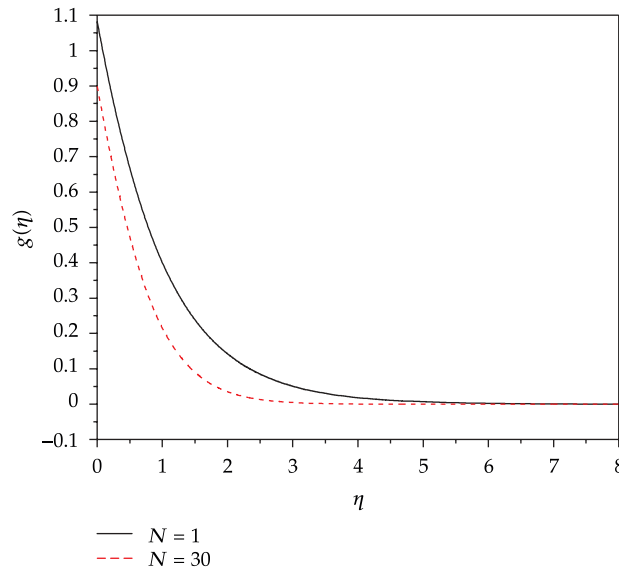


**Figure 19:** The effect of radiation parameter  $N$  on the temperature profile for the PHF case at  $\beta = 0.1$ ,  $Mn = 0.5$ ,  $Ec = 1$ ,  $Pr = 3$ .

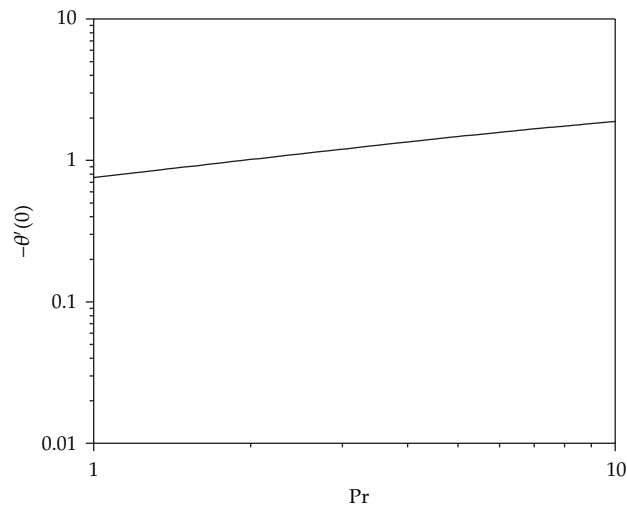


**Figure 20:** Dimensionless heat flux  $-\theta'(0)$  at the sheet versus Prandtl number.

Figures 18 and 19 show the effect of radiation parameter,  $N$ , on the temperature profiles above the sheet. An increase in the radiation parameter decreases fluid temperature for both the PST and PHF cases.

A drop in skin friction as investigated in this paper has an important implication that in free coating operations, elastic properties of the coating formulations may be beneficial for the whole process, which means that less force may be needed to pull a moving sheet at a given withdrawal velocity, or equivalently higher withdrawal speeds can be achieved for a given driving force resulting in increase in the rate of production [32]. A drop in skin friction

with increase in elastic parameter as observed in Table 1 gives the comparison of present results with that of Hayat et al. [24] and Sadeghy et al. [29]. Without any doubt, from this table, we can claim that our results are in excellent agreement with those [24, 29].

## 6. Conclusions

The present work analyses the MHD flow and heat transfer within a boundary layer of UCM fluid above a stretching sheet. Numerical results are presented to illustrate the details of the flow and heat transfer characteristics and their dependence on the various parameters.

- (1) We observe that when the magnetic parameter increases, the velocity decreases; also, for increase in elastic parameter, there are decreases in velocity. The effect of magnetic field and elastic parameter on the UCM fluid above the stretching sheet is to suppress the velocity field, which in turn causes the enhancement of the temperature field.
- (2) Also it is observed that an increase of Prandtl number results in decreasing thermal boundary layer thickness and more uniform temperature distribution across the boundary layer in both the PST and PHF cases. The reason is that smaller values of Pr are equivalent to increasing the thermal conductivities, and therefore heat is able to diffuse away from the heated surface more rapidly than for higher values of Pr.
- (3) An increase in the Eckert number causes an increase in the temperature of the fluid above the sheet. Thus, it may be used to reduce the rate of cooling. For the PST case, fluid temperature near the wall is predicted to exceed wall temperature inferring that the direction of heat transfer is reversed from the fluid to the sheet.
- (4) An increase in the radiation parameter causes a decrease in the temperature of the fluid medium above the sheet. This effect can be used to increase the rate of cooling of the sheet when required.

The dimensionless wall temperature gradient  $-\theta'(0)$  takes a higher value at large Prandtl number Pr. (see Figure 20).

## Nomenclature

- $b$ : Stretching rate [ $s^{-1}$ ]  
 $x$ : Horizontal coordinate [m]  
 $y$ : Vertical coordinate [m]  
 $u$ : Horizontal velocity component [ $ms^{-1}$ ]  
 $v$ : Vertical velocity component [ $ms^{-1}$ ]  
 $T$ : Temperature [K]  
 $t$ : Time [s]  
 $C_p$ : Specific heat [ $J kg^{-1}K^{-1}$ ]  
 $f$ : Dimensionless stream function  
Pr: Prandtl number,  $\nu/k$   
Ec: Eckert number,  $a^2 l^2 / C_p T_s$   
 $N$ : Radiation parameter,  $N = 4\sigma^* T_\infty^3 / k k^*$   
 $M^2$ : Magnetic parameter,  $\sigma B_0^2 / \rho b$   
 $q$ : Heat flux,  $-k(\partial T / \partial y)$  [ $J s^{-1} m^{-2}$ ]

$Nu_x$ : Local Nusselt number, (3.15)

$C_f$ : Skin friction coefficient, (3.16).

### Greek Symbols

$\beta$ : Elastic parameter

$\eta$ : Similarity variable, (2.5)

$\theta$ : Dimensionless temperature

$k$ : Thermal diffusivity [ $\text{m}^2 \text{s}^{-1}$ ]

$\mu$ : Dynamic viscosity [ $\text{kg m}^{-1} \text{s}^{-1}$ ]

$\nu$ : kinematic viscosity [ $\text{m}^2 \text{s}^{-1}$ ]

$\rho$ : Density [ $\text{kg m}^{-3}$ ]

$\tau$ : Shear stress,  $\mu \partial u / \partial y$  [ $\text{kg m}^{-1} \text{s}^{-2}$ ]

$\psi$ : Stream function [ $\text{m}^2 \text{s}^{-1}$ ].

### Subscripts

X: local value.

### Superscripts

' : First derivative

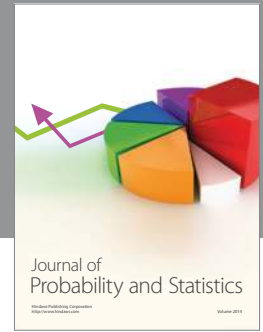
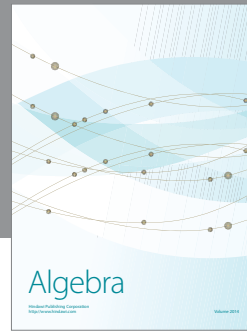
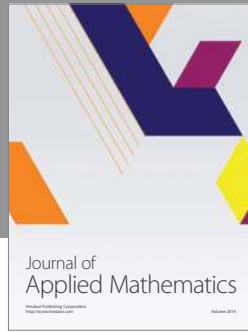
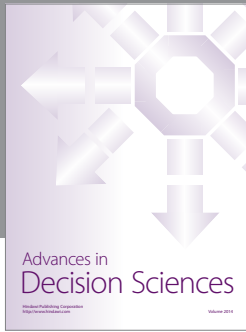
" : Second derivative

''' : Third derivative.

## References

- [1] R. B. Bird, R. C. Armstrong, and O. Hassager, *Dynamics of Polymeric Liquids*, vol. 1, John Wiley & Sons, New York, NY, USA, 1987.
- [2] T. Sarpakaya, "Flow of non-Newtonian fluids in a magnetic field," *AIChE Journal*, vol. 7, pp. 324–328, 1961.
- [3] L. J. Crane, "Flow past a stretching plate," *Zeitschrift für Angewandte Mathematik und Physik*, vol. 21, no. 4, pp. 645–647, 1970.
- [4] L. J. Grubka and K. M. Bobba, "Heat Transfer characteristics of a continuous stretching surface with variable temperature," *Journal of Heat Transfer*, vol. 107, no. 1, pp. 248–250, 1985.
- [5] B. K. Dutta and A. S. Gupta, "Cooling of a stretching sheet in a viscous flow," *Industrial and Engineering Chemistry Research*, vol. 26, no. 2, pp. 333–336, 1987.
- [6] D. R. Jeng, T. C. A. Chang, and K. J. Dewitt, "Momentum and heat transfer on a continuous surface," *ASME Journal of Heat Transfer*, vol. 108, pp. 532–539, 1986.
- [7] C. K. Chen and M. I. Char, "Heat transfer of a continuous, stretching surface with suction or blowing," *Journal of Mathematical Analysis and Applications*, vol. 135, no. 2, pp. 568–580, 1988.
- [8] A. Chakrabarti and A. S. Gupta, "Hydromagnetic flow and heat transfer over a stretching sheet," *Quarterly of Applied Mathematics*, vol. 37, no. 1, pp. 73–78, 1979.
- [9] H. I. Andersson, K. H. Bech, and B. S. Dandapat, "Magnetohydrodynamic flow of a power-law fluid over a stretching sheet," *International Journal of Non-Linear Mechanics*, vol. 27, no. 6, pp. 929–936, 1992.
- [10] N. Afzal, "Heat transfer from a stretching surface," *International Journal of Heat and Mass Transfer*, vol. 36, no. 4, pp. 1128–1131, 1993.
- [11] K. V. Prasad, S. Abel, and P. S. Datti, "Diffusion of chemically reactive species of a non-Newtonian fluid immersed in a porous medium over a stretching sheet," *International Journal of Non-Linear Mechanics*, vol. 38, no. 5, pp. 651–657, 2003.

- [12] M. S. Abel, P. G. Siddheshwar, and M. M. Nandeppanavar, "Heat transfer in a viscoelastic boundary layer flow over a stretching sheet with viscous dissipation and non-uniform heat source," *International Journal of Heat and Mass Transfer*, vol. 50, no. 5-6, pp. 960–966, 2007.
- [13] M. S. Abel and N. Mahesha, "Heat transfer in MHD viscoelastic fluid flow over a stretching sheet with variable thermal conductivity, non-uniform heat source and radiation," *Applied Mathematical Modelling*, vol. 32, no. 10, pp. 1965–1983, 2008.
- [14] J. F. Agassant, P. Avens, and J. Sergent PJ Carreau, *Polymer Processing: Principles and Modelling*, Hanser Publishers, Munich, Germany, 1991.
- [15] K. R. Rajgopal, T. Y. Na, and A. S. Gupta, "Flow of a viscoelastic fluid over a stretching sheet," *Rheologica Acta*, vol. 23, pp. 213–215, 1984.
- [16] H. I. Andersson, "MHD flow of a viscoelastic fluid past a stretching surface," *Acta Mechanica*, vol. 95, no. 1–4, pp. 227–230, 1992.
- [17] D. N. Schulz and J. E. Glass, Eds., *Polymers as Rheology Modifiers*, ACS symposium Series, 462, American Chemical Society, Washington, DC, USA, 1991.
- [18] A. Raptis and C. Perdikis, "Viscoelastic flow by the presence of radiation," *Zeitschrift fur Angewandte Mathematik und Mechanik*, vol. 78, no. 4, pp. 277–279, 1998.
- [19] A. Raptis, "Radiation and viscoelastic flow," *International Communications in Heat and Mass Transfer*, vol. 26, no. 6, pp. 889–895, 1999.
- [20] I. C. Liu, "Flow and heat transfer of an electrically conducting fluid of second grade in a porous medium over a stretching sheet subject to a transverse magnetic field," *International Journal of Non-Linear Mechanics*, vol. 40, no. 4, pp. 465–474, 2005.
- [21] I. C. Liu, "A note on heat and mass transfer for a hydromagnetic flow over a stretching sheet," *International Communications in Heat and Mass Transfer*, vol. 32, no. 8, pp. 1075–1084, 2005.
- [22] P. G. Siddheshwar and U. S. Mahabaleswar, "Effects of radiation and heat source on MHD flow of a viscoelastic liquid and heat transfer over a stretching sheet," *International Journal of Non-Linear Mechanics*, vol. 40, no. 6, pp. 807–820, 2005.
- [23] T. Hayat, Z. Abbas, M. Sajid, and S. Asghar, "The influence of thermal radiation on MHD flow of a second grade fluid," *International Journal of Heat and Mass Transfer*, vol. 50, no. 5-6, pp. 931–941, 2007.
- [24] T. Hayat, Z. Abbas, and M. Sajid, "Series solution for the upper-convected Maxwell fluid over a porous stretching plate," *Physics Letters, Section A*, vol. 358, no. 5-6, pp. 396–403, 2006.
- [25] K. Sadeghy, A. H. Najafi, and M. Saffaripour, "Sakiadis flow of an upper-convected Maxwell fluid," *International Journal of Non-Linear Mechanics*, vol. 40, no. 9, pp. 1220–1228, 2005.
- [26] A. Alizadeh-Pahlavan, V. Aliakbar, F. Vakili-Farahani, and K. Sadeghy, "MHD flows of UCM fluids above porous stretching sheets using two-auxiliary-parameter homotopy analysis method," *Communications in Nonlinear Science and Numerical Simulation*, vol. 14, no. 2, pp. 473–488, 2009.
- [27] M. Renardy, "High Weissenberg number boundary layers for the upper convected Maxwell fluid," *Journal of Non-Newtonian Fluid Mechanics*, vol. 68, no. 1, pp. 125–132, 1997.
- [28] I. J. Rao and K. R. Rajagopal, "On a new interpretation of the classical Maxwell model," *Mechanics Research Communications*, vol. 34, no. 7-8, pp. 509–514, 2007.
- [29] K. Sadeghy, H. Hajibeygi, and S. M. Taghavi, "Stagnation-point flow of upper-convected Maxwell fluids," *International Journal of Non-Linear Mechanics*, vol. 41, no. 10, pp. 1242–1247, 2006.
- [30] A. Alizadeh-Pahlavan and K. Sadeghy, "On the use of homotopy analysis method for solving unsteady MHD flow of Maxwellian fluids above impulsively stretching sheets," *Communications in Nonlinear Science and Numerical Simulation*, vol. 14, no. 4, pp. 1355–1365, 2009.
- [31] V. Aliakbar, A. Alizadeh-Pahlavan, and K. Sadeghy, "The influence of thermal radiation on MHD flow of Maxwellian fluids above stretching sheets," *Communications in Nonlinear Science and Numerical Simulation*, vol. 14, no. 3, pp. 779–794, 2009.
- [32] K. R. Rajagopal, "Boundary Layers in non-Newtonian fluids," M. D. P. Montieivo Marques and J. F. Rodrigues, Eds.
- [33] S. D. Conte and C. de Boor, *Elementary Numerical Analysis*, McGraw-Hill, New York, NY, USA, 1972.
- [34] T. Cebeci and P. Bradshaw, *Physical and Computational Aspects of Convective Heat Transfer*, Springer, New York, NY, USA, 1984.



# Hindawi

Submit your manuscripts at  
<http://www.hindawi.com>

